# OPTICAL EMISSION CHARACTERISTICS OF GUIDED STREAMERS GENERATED IN HELIUM AND ARGON MIXTURES WITH $N_2$ AND $O_2$

K. GAZELI[1, 2], P. SVARNAS[2] AND F. CLEMENT[1]*

[1] IPREM, LCABIE, Plasmas et Applications,
Université de Pau et des Pays de l'Adour, 64000, Pau, France
[2]Electrical and Computer Engineering Department, High Voltage Laboratory,
University of Patras, 26504, Rion-Patras, Greece
*Corresponding author: franck.clement@univ-pau.fr

## ABSTRACT

The optical emission characteristics of Atmospheric Pressure Guided Streamers (APGSs) generated in He and Ar mixtures with $N_2$ and $O_2$, are herein reported. The reactor employed is based on a DBD geometry and driven by high voltage microsecond positive pulses. For fixed values of the main operating parameters, the influence of the gas composition on the formation of principal emissive species as well as on the rotational temperature of probe molecules is investigated. In addition, the vibrational temperature is estimated for both He and Ar mixtures. Optimal gas compositions for enhanced plasma chemistry are found. This is of great importance in various applications and especially biomedical ones. In the latter case the temperature must be maintained close to the room one.

## 1. INTRODUCTION

Atmospheric pressure cold plasma devices operating with noble gases and driven by sinusoidal or pulsed high voltage, have gained great interest in many fields of research such as biomedicine [1]. Up to today, numerous topologies have been suggested for plasma production at atmospheric pressure. As regards the nature of the plasma produced, it is found that it consists of fast travelling streamer-like ionizing waves (APGSs) guided by a dielectric surface and a channel formed by the gas [2,3]. Concerning plasma-surface interactions, the role of reactive oxygen and nitrogen species (ROS and RNS) appears to be dominant. However the contribution of other factors such as plasma-induced heating effects, UV radiation, electric field and charged species must not be disregarded. On the other hand, to achieve enhanced plasma chemistry, small controllable amounts of molecular gases such as $N_2$ and $O_2$ can be mixed uniformly with the main gas (usually He, Ar, Ne, etc.).

The present work is devoted to the investigation of optical emission features of APGS generated in mixtures of He and Ar with $N_2$ and $O_2$. The rotational temperature of probe molecules is measured and the gas temperature as a function of the gas composition remains close to the room one. Additionally, the measurement of the vibrational temperature for He and Ar mixtures provides information on the absorbed energy. These results contribute to the better understanding of the formation and propagation mechanisms of reactive plasma species, and operational windows oriented to biomedical applications are determined.

## 2. EXPERIMENTAL SETUP

*Fig. 1* depicts the configuration of the material used in this study. The reactor employed consists of a quartz tube into which a tungsten micro-wire is inserted. A cylindrical hollow electrode is tightly attached on the outer surface of the tube and grounded directly. The micro-wire is biased by positive HV pulses (kHz range) of steep slopes. Herein the amplitude (*V*) of the voltage is fixed at 7.5 kV, the frequency (*f*) at 10 kHz, and the pulse duty cycle (*d*) at 1%. The applied

voltage is measured through a Tektronix P6015A capacitive divider. The DBD current is recorded with a wideband current transformer (Pearson Electronics 6585) as shown in *Fig. 1*. All signals are monitored simultaneously on a digital oscilloscope (Tektronix TDS3054B, 500 MHz - 5 GS/s).

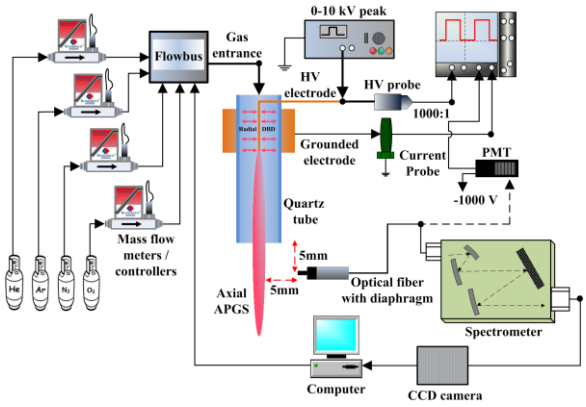


*Fig. 1: Experimental setup of the instruments used.*

In this reactor, due to the coaxial Dielectric Barrier Discharge (DBD) configuration, radial discharges are developed. At the same time, due to the high local electric field at the sharp tip of the micro-wire, APGSs may propagate axially inside and outside the tube, as shown in *Fig. 2*.

High purity (99.999%) He or Ar (carrier gases) is introduced in the tube and ejected in the surrounding atmospheric air. Small $N_2$ and $O_2$ percentages (0.01-0.05 slm, corresponding to 0.49-2.44%) in a total flow rate of 2 slm (100%) are used as additives. The mixtures are precisely adjusted using four mass flow controllers (Bronkhorst High-Tech EL-FLOW) connected to a PC-based flow-bus (see *Fig. 1*).

To estimate the length of the APGS luminous propagation path (wavelength-integrated measurements in the UV-visible region), a photomultiplier tube (PMT, Hamamatsu R928) is used as light detector (see *Fig. 1*).

Emissive species (wavelength-resolved measurements in the UV-visible region) are identified by optical emission spectroscopy (OES). To collect the APGS emitted light, an optical fiber (Ceramoptec UV1500/1590N) is alternatively connected either to the aforementioned PMT or a spectrometer (1000M JOBIN YVON, grating of 1200 grooves/mm, blazed at 500 nm) which is equipped with a CCD 3000V camera. Finally, in order to compare species intensities, special attention is paid for the interpretation of the relative OES intensities, by calibrating the spectroscopic system appropriately.

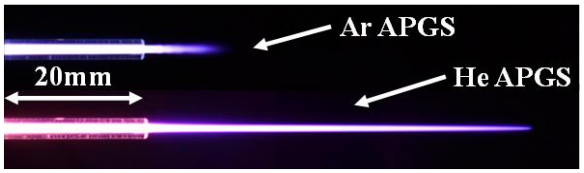


*Fig. 2: Variation of the APGS visible pattern for pure Ar and He gas (Q=2 slm, V=7.5 kV, f=10 kHz, and d=1%).*

The influence of the gas composition on the visible pattern of the APGS is observed by capturing high resolution photos (*Fig. 2*). A Nikon D3100 camera is used with the following settings: ISO 100, f/5.6, and exposure time 30 s.

## 3. RESULTS AND DISCUSSION

*Fig. 2* compares the APGS pattern generated under pure Ar and He conditions. At a glance, it appears that for He a longer propagation path is achieved (~45 mm). In the case of Ar the path is clearly shorter and it obtains a length of about 10 mm. Furthermore, the different colours of the plasma produced for Ar and He are distinguishable. Despite the clear qualitative character of these observations, they imply different propagation mechanisms and plasma chemistries for each gas. This fact is established below by OES.

Another important factor that determines the plasma visible pattern is the gas flow profile. The APGS propagation is favorized by a laminar flow whereas it is prevented by a turbulent flow [4]. An intermediate flow corresponds to a transitional regime. Although the plasma activation can highly modify the flow profile of the neutral gas [4], a first indication on the flow profile can be obtained by the dimensionless Reynolds number ($Re = \rho\ Q\ D\ /\ A\ \mu$) [5]. In this expression, $\rho$ is the gas density (0.16039 $kgm^{-3}$ for He [6] and 1.6228 $kgm^{-3}$ for Ar [5], at room temperature and atmospheric pressure), $Q$ is the gas flow rate in $m^3s^{-1}$ (herein 2 slm = $3.333x10^{-5}$ $m^3s^{-1}$), $D$ is the tube diameter ($1x10^{-3}$ m), $A$ is the tube cross-sectional area [3.14 x $(D/2)^2$], and $\mu$ is the dynamic viscosity of the gas ($1.991x10^{-5}$ $Nsm^{-2}$ for He [6] and $2.125x10^{-5}$ $Nsm^{-2}$ for Ar [5]). This simple calculation gives $Re$=345 for He and $Re$=3237 for Ar, and according to [7], the flow is laminar in the He case and transitional in the Ar case. These different flow regimes may

explain the discrepancies observed on the patterns of *Fig. 2*.

Among all reactive species generated in atmospheric pressure plasmas, NO, OH, and O radicals play an important role in the plasma-based processes. The OES intensity of dominant species emitting in the wide spectrum 300-900 nm as a function of He and Ar mixtures is plotted in *Fig. 3* and *Fig. 4*, respectively. For both carrier gases, apart from their atomic lines, emissions from OH, $N_2$(SPS), and O are detected. Especially for the He case, $N_2^+$(FNS) is present in the emission spectrum. In addition, bands of $NO_\gamma$ and $N_2$(FPS) have been detected with weaker intensities (not presented here).

Regarding the He-$N_2$ mixtures (*Fig. 3(a)*), when pure He is used He (667 nm and 706 nm) and O (777 nm) are maximized and they decrease as far as $N_2$ is added. On the other hand, OH (309 nm), $N_2$(SPS) (337 nm), and $N_2^+$(FNS) (391 nm) exhibit an optimum around 0.49% of $N_2$.

Concerning He-$O_2$ mixtures (*Fig. 3(b)*) the intensity of all species decays versus $O_2$ percentage.

For the Ar-$N_2$ mixtures (*Fig. 4(a)*), the Ar (794 and 811 nm), OH (309 nm), and O (777 nm) intensities are maximal for pure Ar and they decrease as far as $N_2$ is added. In contrast, the $N_2$(SPS) (337 nm) increases monotonously for $N_2$ percentage up to 2.44%. As the concentration of $N_2$ is increased, the collisional cross-section of $N_2$ molecules also increases, leading to intense $N_2$ excited states. Apart from electron impact, $N_2$(SPS) can be populated through $N_2$ collisions with Ar metastables. Finally, regarding the mixtures of Ar-$O_2$ (*Fig. 4(b)*), similar tendencies with those presented in *Fig. 3(b)* are obtained.

To estimate the gas temperature, the recorded rotational distributions of two probe molecules, i.e. OH ($A^2\Sigma^+(0)$-$X^2\Pi(0)$ at 309 nm) and $N_2$(SPS) ($C^3\Pi_u(0)$-$B^3\Pi_g(0)$ at 337.1 nm), are fitted to the theoretical ones using a home-built software [8]. The rotational temperature ($T_{rot}$) varies between 300 and 350 K for every gas mixture. As regards the overall temperature of the neutral gas, it can fairly be assumed low enough for biomedical applications, due to the rather low values of the $T_{rot}$ and the extremely low duty cycle of the voltage applied ($d$=1%). Hence, electrical energy delivery and gas heating take place during a very short fraction of the pulse period, while during the main part of the period the gas cools down.

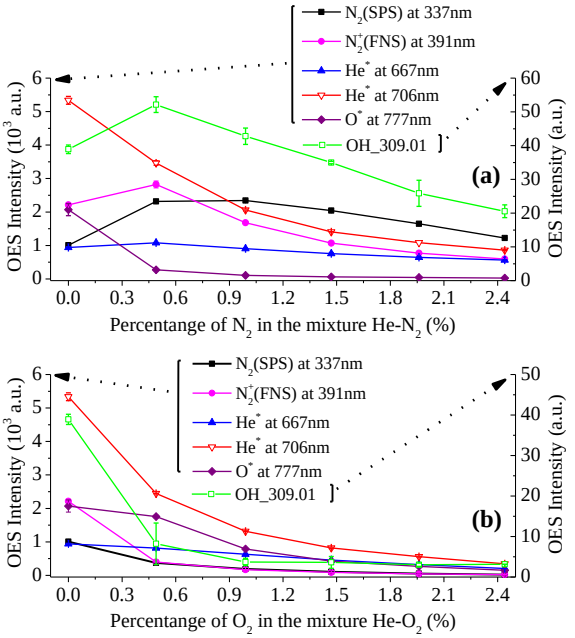


*Fig. 3: OES relative intensities of principal emissive species as a function of (a) $N_2$ and (b) $O_2$ percentage in He.*

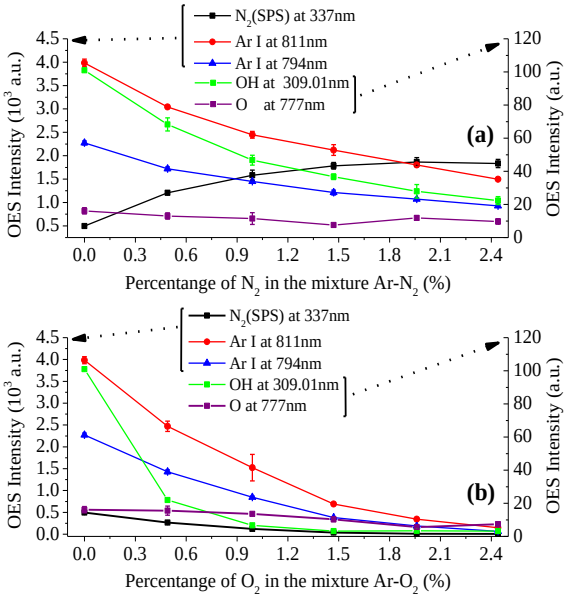


*Fig. 4: OES relative intensities of principal emissive species as a function of (a) $N_2$ and (b) $O_2$ percentage in Ar.*

Finally, the vibrational temperature ($T_{vib}$) is calculated for pure He and Ar in the inter-diffusion with air region (see *Fig. 1*). This can provide valuable information about the electron energy transfer to molecules and is related to energy accumulation in the plasma. Herein, $T_{vib}$ is estimated from the Boltzmann's plots [9] corresponding to the $N_2(C^3\Pi_u$-$B^3\Pi_g)$ vibrational transitions. The emission range 365-400 nm ($\Delta\upsilon$=-2) is considered (see *Fig. 5*).

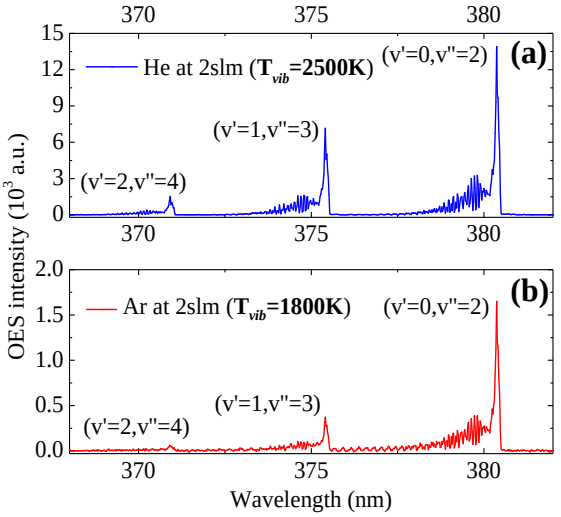


*Fig. 5: Typical vibrational bands of $N_2$(SPS, $\Delta\upsilon$=-2) used for the calculation of the vibrational temperature in pure (a) He and (b) Ar discharge.*

When pure He or Ar is used, the vibrational temperature of the probed nitrogen molecules due to the air equals to about 2500 K and 1800 K, respectively. This difference indicates that less energy is transferred in the Ar case. This is reflected as well on the optical emission spectra where more intense vibrational transitions are recorded in the case of He (see *Fig. 5*). The APGS propagation may also be affected by this fact, as illustrated in *Fig. 2* where shorter propagation path is obtained for Ar gas as compared with that of He.

## 4. CONCLUSION

In this work, a DBD reactor was presented for the generation of APGSs in mixtures of He-$N_2$ & He-$O_2$ and Ar-$N_2$ & Ar-$O_2$. Pulsed positive high voltage was used. The effect of gas composition on the plasma pattern, OES spectra, rotational and vibrational temperatures was investigated. The gas flow was characterized as laminar for He, while it appeared to be in transitional mode for Ar. Copious reactive species were detected in the optical emission spectra and optimal gas compositions were determined for enhanced plasma chemistry. Among the various species identified, radicals like NO, OH, and O are of great importance for biomedical applications. At the same time, the average gas temperature was measured close to the room one. Finally, the vibrational temperature of nitrogen molecules in the air, where the streamers were propagated, was found smaller in the Ar case than in the He one, possibly related to less energy transfer in Ar discharges.

## REFERENCES

[1] G. E. Morfill, M. G. Kong, J. L. Zimmermann, "Focus on Plasma Medicine", New J. Phys. 11, 115011, 2009

[2] J.-P. Boeuf, L. L. Yang, L. C. Pitchford, "Dynamics of a guided streamer (‘plasma bullet’) in a helium jet in air at atmospheric pressure", J. Phys. D.: Appl. Phys. 46, 015201, 2013

[3] K. Gazeli, P. Svarnas, P. Vafeas, P. K. Papadopoulos, A. Gkelios, F. Clément, "Investigation on streamers propagating into a helium jet in air at atmospheric pressure: Electrical and optical emission analysis", J. Appl. Phys. 114, 103304, 2013

[4] J.-S. Oh, O. T. Olabanji, C. Hale, R. Mariani, K. Kontis and J. W. Bradley, "Imaging gas and plasma interactions in the surface-chemical modification of polymers using micro-plasma jets", J. Phys. D: Appl. Phys. 44, 155206, 6pp, 2011

[5] X. J. Shao, G.-J. Zhang, J.-Y. Zhan, H.-B. Mu, "Investigation on Spurt Length of Atmospheric-Pressure Plasma Jets", IEEE Trans. Plasma Sci. 39, 2340–2341, 2011

[6] H. Petersen, *The properties of Helium: Density, Specific Heats, Viscosity, and Thermal Conductivity at Pressures from 1 to 100 bar and from Room Temperature to about 1800 K*, Danish Atomic Energy Commission Research Establishment Risö (Risö Report No. 224), 1970.

[7] Yunus A. Çengel, John M. Cimbala / *Fluid mechanics: Fundamentals and applications—1st ed. p. cm.* — (McGraw-Hill series in mechanical engineering) ISBN 0–07–247236–7

[8] R. P. Cardoso, T. Belmonte, P. Keravec, F. Kosior and G. Henrion, "Influence of impurities on the temperature of an atmospheric helium plasma in microwave resonant cavity", J. Phys. D: Appl. Phys. 40, 1394-1400, 2007

[9] X. Lu, Z. Jiang, Q. Xiong, Z. Tang, Y. Pan, "A single electrode room-temperature plasma jet device for biomedical applications", Appl. Phys. Lett. 92, 151504, 2008